Macroscopic Einstein-Podolsky-Rosen pairs in superconducting circuits

L. F. Wei,[1,2] Yu-xi Liu,[1] Markus J. Storcz,[1,3] and Franco Nori[1,4]
[1]*Frontier Research System, The Institute of Physical and Chemical Research (RIKEN), Wako-shi, Saitama, 351-0198, Japan*
[2]*Institute of Quantum Optics and Quantum Information, Department of Physics, Shanghai Jiaotong University, Shanghai 200030, P.R. China*
[3]*Physics Department, ASC, and CeNS, Ludwig-Maximilians-Universität, Theresienstrasse 37, 80333 München, Germany*
[4]*Center for Theoretical Physics, Physics Department, CSCS, The University of Michigan, Ann Arbor, Michigan 48109-1040, USA*
(Received 15 August 2005; published 9 May 2006)

We propose an efficient approach to prepare Einstein-Podolsky-Rosen (EPR) pairs in currently existing Josephson nanocircuits with capacitive couplings. In these fixed coupling circuits, two-qubit logic gates could be easily implemented while, strictly speaking, single-qubit gates cannot be easily realized. For a known two-qubit state, conditional single-qubit operation could still be designed to evolve only the selected qubit and keep the other qubit unchanged; the rotation of the selected qubit depends on the state of the other one. These conditional single-qubit operations allow us to deterministically generate the well-known Einstein-Podolsky-Rosen pairs, represented by EPR-Bell (or Bell) states. Quantum-state tomography is further proposed to experimentally confirm the generation of these states. The decays of the prepared EPR pairs are analyzed using numerical simulations. Possible application of the generated EPR pairs to test Bell's Inequality is also discussed.

DOI: 10.1103/PhysRevA.73.052307 PACS number(s): 03.67.Mn, 03.65.Wj, 85.25.Dq

I. INTRODUCTION

Quantum mechanics (QM) is a very successful theory. It has solved many physical mysteries in both macroscopic superconductivity and microscopic particles. Still, laboratory studies of its conceptual foundation and interpretation continue to attract much attention. One of the most important examples is the well-known Einstein-Podolsky-Rosen (EPR) "paradox," concerning the completeness of QM. Based on a *gedanken* experiment, Einstein, Podolsky, and Rosen (EPR) claimed [1] that QM is incomplete and that so-called "hidden variables" should exist. This is because a two-particle quantum system might be prepared in a correlated (i.e., entangled) state, even though the two particles are spatially separated by a large distance and without any direct interaction. A measurement performed on one of the particles immediately changes the state (and thus the possible physical outcome) of the other particle. This paradox leads to much subsequent, and still on going, researches. Bell proposed [2] an experimentally testable inequality to examine the existence of the hidden variables: if this inequality is violated, then there are no so-called local "hidden variables," and thus quantum mechanical predication of existing quantum nonlocal correlations (i.e., entanglement) is sustained.

During the past decades, a number of interesting experiments [3] using entangled photon pairs have been proposed and carried out to investigate the two-particle nonlocal correlations. These experiments showed that Bell's inequality (BI) could be strongly violated, and agreed with quantum mechanical predictions. Yet, one of the essential loopholes in these optical experiments is that the required EPR pairs were probabilistically generated in a small subset of all photons created in certain spontaneous processes. Thus, it is necessary to study two-particle entanglement in different, e.g., massive or macroscopic systems, instead of fast-escaping photons. Expectably, the EPR pairs between these massive "particles" can be deterministically prepared. Theoretical proposals include those with e.g., neutral kaons [4], Rydberg atoms [5], ballistic electrons in semiconductors [6], and trapped ions [7]. Experimentally, two Rydberg atoms had been first entangled to form EPR pair in a high Q cavity by the exchange of a single photon [8]. Later, by exchanging the quanta of the common vibrational mode, EPR correlations with ultralong lifetime (e.g., up to 5 μs) had been generated between a pair of trapped cold ions [9]. Consequently, violations of BI have been experimentally verified with the EPR correlations between either the two ions [10], or an atom and a photon [11].

Recent developments of quantum manipulation in coupled Josephson systems [12,13] allow us to experimentally investigate the quantum correlations between two macroscopic degrees of freedom in a superconducting nanoelectronic device [14]. Proposals have been made for producing quantum entanglement between two superconducting qubits, e.g., indirectly coupled by sequentially interacting with a current-biased information bus [15,16], coupled inductively [17,18], and coupled via either a cavity mode [19], or a large Josephson junction [20]. By introducing an effective dynamical decoupled approach, we have shown [21] that the BI could also be tested with superconducting qubits, even if the interaction between them is fixed. The robustness of the scheme proposed in Ref. [21] is better suited for weak interbit couplings, e.g., when the ratio of the interbit-coupling energy E_m and the Josephson energy E_J of the qubit is small. In this paper, for *an arbitrary interbit coupling* strength, we discuss how to prepare the EPR correlations, i.e., deterministically generate and tomographically measure the well-known EPR-Bell (or Bell) states

$$|\psi_{\pm}\rangle = \frac{1}{\sqrt{2}}(|00\rangle \pm |11\rangle), \quad |\phi_{\pm}\rangle = \frac{1}{\sqrt{2}}(|01\rangle \pm |10\rangle), \qquad (1)$$

in a capacitively coupled Josephson circuit. Its possible application to directly test the EPR paradox is also discussed.

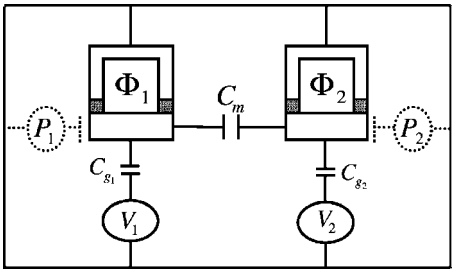

FIG. 1. Two capacitively-coupled SQUID-based charge qubits. The quantum states of two Cooper-pair boxes (i.e., qubits) are manipulated by controlling the applied gate voltages V_1, V_2 and external magnetic fluxes Φ_1, Φ_2 (threading the SQUID loops). P_1 and P_2 (dashed line parts) read out the final qubit states.

The outline of the paper is as follows. In Sec. II, a few elementary quantum operations are proposed to deterministically manipulate two charge qubits coupled capacitively. Some of them only evolve a selected qubit and leave the remaining one unaffected. These operations are not strictly single-qubit gates (just *conditional* single-qubit operations), as the rotation of the selected qubit depends on the state of the other qubit. By making use of these operations, in Sec. III, we propose a two step approach to deterministically generate the EPR pairs from the circuit's ground state $|\psi(0)\rangle = |00\rangle$. Further, we discuss how to experimentally confirm the generation of EPR pairs by tomographic measurements. In Sec. IV, considering the existence of typical voltage noises and $1/f$ noise, we numerically analyze the decays of the prepared EPR correlations within the Bloch-Redfield formalism [22]. In Sec. V, we discuss the possibility of testing BI with the generated EPR pairs. Conclusions and discussions are given in Sec. VI.

II. MANIPULATIONS OF TWO CAPACITIVELY COUPLED JOSEPSHON CHARGE QUBITS

We consider the two-qubit nanocircuit sketched in Fig. 1, which is similar to that in recent experiment [12,23]. Two superconducting quantum interference device (SQUID) loops with controllable Josephson energies produce two Cooper-pair boxes, fabricated a small distance apart [12,23]) and coupled via the capacitance C_m. The Hamiltonian of the circuit reads

$$\hat{H} = \sum_{j=1,2} [E_{C_j}(\hat{n}_j - n_{g_j})^2 - E_J^{(j)} \cos \hat{\theta}_j] + E_m \prod_{j=1}^{2} (\hat{n}_j - n_{g_j}), \tag{2}$$

in the charge basis. Here, the excess Cooper-pair number operator $\hat{n}_j$ and phase operator $\hat{\theta}_j$ in the jth box are conjugate: $[\hat{\theta}_j, \hat{n}_k] = i\delta_{jk}$. $E_{C_j} = 4e^2 C_{\Sigma_k}/C_\Sigma$, $j \neq k = 1,2$, and $E_J^{(j)} = 2\varepsilon_{J_j} \cos(\pi\Phi_j/\Phi_0)$ are the charging and Josephson energies of the jth box. $E_m = 4e^2 C_m/C_\Sigma$ is the coupling energy between the boxes. Above, ε_{J_j} and C_{Σ_j} are the Josephson energy of the single junction and the sum of all capacitances connected to the jth box, respectively. Also, $C_\Sigma = C_{\Sigma_1} C_{\Sigma_2} - C_m^2$ and $n_{g_j} = C_{g_j} V_j/(2e)$. e is the electron charge and Φ_0 the flux quantum. The circuit works in the charge regime with $k_B T \ll \varepsilon_{J_j} \ll E_{C_j} \ll \Delta$, wherein quasiparticle tunneling and excitation are effectively suppressed and the number n_j (with $n_j = 0, 1, 2, \ldots$) of Cooper-pairs in the jth box is a good quantum number. Here, k_B, T, Δ, and $2\varepsilon_{J_j}$ are the Boltzmann constant, temperature, superconducting gap, and maximal Josephson energies of the jth Cooper-pair box, respectively.

Following Refs. [12,23], the dynamics of the system near the coresonance point (where $n_{g_1} = n_{g_2} = 1/2$) can be effectively restricted to the subspace Ξ spanned by only the four lowest charge states: $|00\rangle$, $|10\rangle$, $|01\rangle$, and $|11\rangle$, and thus the above Hamiltonian can be simplified to

$$\hat{H} = \sum_{j=1,2} \frac{1}{2}[E_C^{(j)} \sigma_z^{(j)} - E_J^{(j)} \sigma_x^{(j)}] + E_{12} \sigma_z^{(1)} \sigma_z^{(2)}, \tag{3}$$

with $E_{12} = E_m/4$, and $E_C^{(j)} = E_{C_j}(n_{g_j} - 1/2) + E_m(n_{g_k}/2 - 1/4)$, $j \neq k = 1,2$. The pesudospin operators are defined as $\sigma_z^{(j)} = |0_j\rangle\langle 0_j| - |1_j\rangle\langle 1_j|$ and $\sigma_x^{(j)} = |0_j\rangle\langle 1_j| + |1_j\rangle\langle 0_j|$. Here, the subindex j (or k) is introduced to label the state of the jth (or kth) qubit. For example, $|0_j\rangle$ refers to the logic state of the jth qubit is "0." For simplicity, the subindexes in a two-qubit state $|mn\rangle$ (with $m,n = 0,1$) are omitted, and $m(n)$ usually (except when indicated otherwise) refers to the state $|m\rangle$ ($|n\rangle$) of the first (second) qubit.

Obviously, the interbit-coupling energy $E_{12} = E_m/4$ is determined by the coupling capacitance C_m and therefore is fixed by fabrication, i.e., not controllable. However, $E_C^{(j)}$ and $E_J^{(j)}$ can be controlled by adjusting the applied gate voltages V_j and fluxes Φ_j, respectively. Although any evolution of this two-qubit system is solvable and can be expressed by a 4×4 matrix in the subspace Ξ, we prefer certain relatively simple quantum operations by properly setting the above controllable parameters to conveniently engineer arbitrary quantum states. These operations are summarized in the following three subsections.

A. Operational delay

First, we assume the circuit stays in the parameter settings such that $E_C^{(j)} = E_J^{(j)} = 0$, until any operation is applied to it. Thus, during the operational delay τ, the circuit evolves under the Hamiltonian $\hat{H}_{\text{int}} = E_{12} \sigma_z^{(1)} \sigma_z^{(2)}$, i.e., undergoes a free time evolution

$$\hat{U}_0 = \begin{pmatrix} e^{-i\alpha_0} & 0 & 0 & 0 \\ 0 & e^{i\alpha_0} & 0 & 0 \\ 0 & 0 & e^{i\alpha_0} & 0 \\ 0 & 0 & 0 & e^{-i\alpha_0} \end{pmatrix}, \quad \alpha_0 = \frac{E_{12}}{\hbar}\tau. \tag{4}$$

In this case, the Bell states in Eq. (1) will not evolve, once they have been generated.

B. Simultaneously evolving two qubits

Due to the constant coupling, simultaneous operations on two qubits are relatively easy. For example, if $n_{g_1} = n_{g_2}$

$=1/2$ (i.e., at coresonance point) and $E_J^{(1)}=E_J^{(2)}=E_J$, then the circuit has the Hamiltonian $\hat{H}_{\rm co}=-E_J(\sigma_x^{(1)}+\sigma_x^{(2)})/2+E_{12}\sigma_z^{(1)}\sigma_z^{(2)}$, which produces the following time-evolution operator

$$\bar{U}_{\rm co}=\frac{1}{2}\begin{pmatrix} a & b & b & c \\ b & a^* & c^* & b \\ b & c^* & a^* & b \\ c & b & b & a \end{pmatrix}, \tag{5}$$

with

$$\begin{cases} a=\cos(t\Omega/\hbar)-iE_{12}\sin(t\Omega/\hbar)/\Omega+\exp(-itE_{12}/\hbar), \\ b=iE_J\sin(t\Omega/\hbar)/\Omega, \quad \Omega=(E_J^2+E_{12}^2)^{1/2}, \\ c=\cos(t\Omega/\hbar)-iE_{12}\sin(t\Omega/\hbar)/\Omega-\exp(-itE_{12}/\hbar). \end{cases}$$

The subindex "co" refers to "coresonance." Thus, we can simultaneously flip the two qubits, i.e., $|00\rangle \rightleftarrows |11\rangle$, and $|01\rangle \rightleftarrows |10\rangle$, by setting the duration as $\cos(t\Omega/\hbar)=-\cos(tE_{12}/\hbar)=1$. Another specific two-qubit quantum operation

$$\hat{U}_{\rm co}=\frac{1}{2}\begin{pmatrix} 1-i & 0 & 0 & 1+i \\ 0 & 1+i & 1-i & 0 \\ 0 & 1-i & 1+i & 0 \\ 1+i & 0 & 0 & 1-i \end{pmatrix} \tag{6}$$

can also be implemented, if the duration is set as $\cos(t\Omega/\hbar)=\sin(tE_{12}/\hbar)=1$.

C. Conditional rotations of a selected qubit

Without the interaction free subspaces [24], a strict single-qubit gate cannot, in principle, be achieved in the system with strong fixed interbit coupling. Recently, we have proposed an effective approach to approximately implement expected single-qubit logic operations [21]. In what follows we show that *conditional* single-qubit operations, i.e., evolving only one selected qubit and leaving the other one unaffected, are still possible. For example, one can set $E_C^{(k)}=E_J^{(k)}=0$ to only rotate the jth qubit. Indeed, the reduced Hamiltonian $\hat{H}_{CJ}^{(j)}=E_C^{(j)}\sigma_z^{(j)}/2-E_J^{(j)}\sigma_x^{(j)}/2+E_{12}\sigma_z^{(1)}\sigma_z^{(2)}$ yields the following time evolution:

$$\bar{U}_{\rm CJ}^{(j)}=\hat{A}_+^{(j)}\otimes|0_k\rangle\langle 0_k|+\hat{A}_-^{(j)}\otimes|1_k\rangle\langle 1_k|, \tag{7}$$

with

$$\begin{gathered} \hat{A}_\pm^{(j)}=\mu_\pm^{(j)}|0_j\rangle\langle 0_j|+\mu_\pm^{(j)*}|1_j\rangle\langle 1_j|+\nu_\pm^{(j)}\sigma_x^{(j)}, \\ \mu_\pm^{(j)}=\cos(t\lambda_\pm^{(j)}/\hbar)-i\cos\alpha_\pm^{(j)}\sin(t\lambda_\pm^{(j)}/\hbar), \\ \nu_\pm^{(j)}=i\sin\alpha_\pm^{(j)}\sin(t\lambda_\pm^{(j)}/\hbar), \quad \sin\alpha_\pm^{(j)}=E_J^{(j)}/(2\lambda_\pm^{(j)}), \\ \lambda_\pm^{(j)}=\sqrt{[E_C^{(j)}/2\pm E_{12}]^2+[E_J^{(j)}/2]^2}. \end{gathered}$$

This implies that, if the kth qubit is in the state $|0_k\rangle$ ($|1_k\rangle$), then the jth qubit undergoes a rotation $\hat{A}_+^{(j)}$ ($\hat{A}_-^{(j)}$). During this operation the kth qubit is unchanged and kept in its initial state. Obviously, if $E_C^{(j)}=2E_{12}$ is satisfied beforehand (thus $\cos\alpha_-^{(j)}=0$), and the duration is set as $\cos(t\lambda_j/\hbar)=1$, $\lambda_j=[(2E_{12})^2+(E_J^{(j)}/2)]^{1/2}$, then the following two-qubit Deutsch gate [25]:

$$\hat{U}_+^{(j)}(\theta_j)=\hat{I}_j\otimes|0_k\rangle\langle 0_k|+[\hat{I}_j\cos\theta_j+i\sigma_x^{(j)}\sin\theta_j]|1_k\rangle\langle 1_k|, \tag{8}$$

with $\theta_j=tE_J^{(j)}/(2\hbar)$, is obtained. Above, $\hat{I}_j$ is the unit operator relating to the jth qubit. The above operation implies that the target qubit (here it is the jth one) undergoes a quantum evolution, only if the control qubit (here, the kth one) is in the logical state "1." If the duration is set to simultaneously satisfy the two conditions: $\sin\theta_j=1$ and $\cos(t\lambda_j/\hbar)=1$, then the above two-qubit operation is equivalent to the well-known controlled-NOT (CNOT) gate, apart from a phase factor. On the other hand, if $E_C^{(j)}=-2E_{12}$ is set beforehand, then the target qubit undergoes the same evolution only if the control qubit is in the logic state "0." The corresponding time-evolution operator reads

$$\hat{U}_-^{(j)}(\theta_j)=\hat{I}_j\otimes|1_k\rangle\langle 1_k|+[\hat{I}_j\cos\theta_j+i\sigma_x^{(j)}\sin\theta_j]|0_k\rangle\langle 0_k|. \tag{9}$$

Furthermore, if $E_C^{(1)}=E_C^{(2)}=E_J^{(k)}=0$ is set beforehand, then the above conditional operation (7) on the jth qubit (keeping the kth one unchanged) reduces to

$$\bar{U}_{\rm J}^{(j)}=\hat{B}_j\otimes|0_k\rangle\langle 0_k|+\hat{B}_j^*\otimes|1_k\rangle\langle 1_k|+\xi_j\sigma_x^{(j)}\otimes\hat{I}_k, \tag{10}$$

with

$$\begin{gathered} \hat{B}_j=\zeta_j|0_j\rangle\langle 0_j|+\zeta_j^*|1_j\rangle\langle 1_j|, \\ \zeta_j=\cos(t\gamma_j/\hbar)-i\cos\alpha_j\sin(t\gamma_j/\hbar), \\ \xi_j=i\sin\alpha_j\sin(t\gamma_j/\hbar), \quad \cos\alpha_j=E_{12}/\gamma_j, \\ \gamma_j=\sqrt{(E_{12})^2+(E_J^{(j)}/2)^2}. \end{gathered}$$

This operation can be further engineered to

$$\hat{U}_{\rm J}^{(j)}=\frac{i}{\sqrt{2}}[-\sigma_z^{(j)}\sigma_z^{(k)}+\sigma_x^{(j)}\otimes\hat{I}_k], \tag{11}$$

if $E_J^{(j)}=2E_{12}$ and $\sin(\gamma_j t/\hbar)=1$ are further set. This is a Hadamard-like operation on the jth qubit.

Of course, the above operations, although they only evolve the selected qubit and leave the other one unaffected, are not the strict single-qubit quantum gates (but just the special two-qubit quantum operations). This is because the rotations of the selected qubit depend on the states of the other one. Note that, due to the presence of the constant interbit coupling E_{12}, the value of $E_C^{(j)}$ depends on both gate voltages applied to the two Cooper-pair boxes. For example, $E_C^{(2)}=0$ requires that the two gate voltages should be set to satisfy the condition: $(n_{g_2}-1/2)/(n_{g_1}-1/2)=-2E_{12}/E_{C_2}$.

III. EPR-BELL STATES: THEIR GENERATIONS AND MEASUREMENTS

Now, it will be shown how to deterministically generate EPR correlations between the above two capacitively

coupled Josephson qubits. We will also propose how to experimentally confirm the expected EPR-Bell states.

A. Deterministic preparations

Naturally, we begin with the ground state of the circuit $|\psi(0)\rangle=|00\rangle$, which can be easily initialized by letting the circuit work far from the coresonance point via a large voltage bias.

First, we prepare the superposition of two logical states of a selected qubit, e.g., the first one. This can be achieved by simply using a pulse of duration t_1 to implement the above quantum operation (9), i.e.

$$|\psi(0)\rangle=|00\rangle \overset{\hat{U}_{-}^{(1)}(\theta_1)}{\rightarrow} |\Psi_{\pm}\rangle=\frac{1}{\sqrt{2}}(|00\rangle \pm i|10\rangle). \tag{12}$$

Here, the duration is set to satisfy the conditions $\cos(t_1\lambda_1/\hbar)=1$ and $\sin\theta_1=\pm 1/\sqrt{2}$. The plus sign corresponds to the time durations for $\theta_1=\pi/4$, and $3\pi/4$. The minus sign corresponds to $\theta_1=5\pi/4$, and $7\pi/4$.

We next conditionally flip the second qubit, keeping the first one unchanged. The expected operations can be simply expressed as either $|00\rangle\rightarrow|01\rangle$, keeping $|10\rangle$ unchanged, or $|10\rangle\rightarrow|11\rangle$, keeping $|00\rangle$ unchanged. The former (latter) operation requires to flip the second qubit if and only if the first qubit is in logic state 0 (1). These manipulations have been proposed above, and thus the desirable Bell states can be deterministically prepared by

$$|\Psi_{\pm}\rangle \overset{\hat{U}_{-}^{(2)}(\theta_2)}{\rightarrow} |\phi_{\pm}\rangle=\frac{1}{\sqrt{2}}(|01\rangle \pm |10\rangle), \tag{13}$$

and

$$|\Psi_{\pm}\rangle \overset{\hat{U}_{+}^{(2)}(\theta_2)}{\rightarrow} |\psi_{\pm}\rangle=\frac{1}{\sqrt{2}}(|00\rangle \pm |11\rangle), \tag{14}$$

respectively. The duration t_2 of the second pulse is determined by the condition $\cos(\lambda_2 t_2/\hbar)=\sin\theta_2=1$.

B. Tomographic reconstructions

The fidelity of the EPR correlations generated above can be experimentally measured by quantum-state tomography, a technique for reconstructing the density matrix of quantum state. For the complete characterization of an unknown two-qubit state with a 4×4 density matrix $\rho=(\rho_{ij,kl})$ (with i, j, k, $l=0,1$), we need to determine 15 independent real parameters, due to $\mathrm{tr}\,\rho=\Sigma_{i,j=0,1}\rho_{ij,ij}=1$, and $\rho_{ij,kl}=\rho^{*}_{kl,ij}$. This can be achieved by a series of measurements on a sufficient number of identically prepared copies. The operations presented above for the generation of EPR pairs could provide enough copies of any expected EPR pairs to be reconstructed. Experimentally, Bell states of pseudo-spins (e.g., in nuclear magnetic resonance systems [26], two-level trapped cold ions [9], and the photon pairs [27]) have been tomographically reconstructed by only using a series of single-qubit manipulations. Recently, we have proposed a generic approach to tomographically measure solid-state qubits with switchable interactions [28]. Due to the relatively strong interbit coupling, which is always on in the circuits considered here, specific operations are required to realize the tomographic reconstruction of the EPR pairs generated.

The state of a charge qubit is often read out by capacitively coupling a single-electron transistor (SET) to the measured qubit [29]. When a projective measurement $\hat{P}_j=|1_j\rangle\langle 1_j|$ is performed on the state ρ, a dissipative current $I_c^{(j)}\propto\mathrm{tr}(\rho\hat{P}_j)$ flows through the jth SET coupled to the jth qubit. Such a projective measurement is equivalent to the measurement of $\sigma_z^{(j)}$, as $\sigma_z^{(j)}=(\hat{I}-\hat{P}_j)/2$. For the present system one may perform three kinds of projective measurements: (i) the P_1 measurement (with projective operator $\hat{P}_1$) acting only on the first qubit (independent of the state of the second qubit); (ii) the P_2 measurement (with projective operator $\hat{P}_2$) operating only on the second qubit (independent of the state of the first qubit); and (iii) the P_{12} measurement (with projective operator $\hat{P}_1\otimes\hat{P}_2$) simultaneously acting on both Cooper-pair boxes.

All diagonal elements of the density matrix ρ can be directly determined by performing these three kinds of projective measurements on the system. In fact, $\rho_{11,11}$ can be determined by the P_{12} measurement as

$$I_c^{(12)}\propto\rho_{11,11}=\mathrm{tr}(\rho\hat{P}_1\otimes\hat{P}_2). \tag{15}$$

Next, $\rho_{10,10}$ could be determined by P_1 measurement as

$$I_c^{(1)}\propto\rho_{10,10}+\rho_{11,11}=\mathrm{tr}(\rho\hat{P}_1). \tag{16}$$

Also, we can determine $\rho_{01,01}$ by the P_2 measurement as

$$I_c^{(2)}\propto\rho_{01,01}+\rho_{11,11}=\mathrm{tr}(\rho\hat{P}_2). \tag{17}$$

The remaining element $\rho_{00,00}$ could be determined by the normalization condition $\mathrm{tr}\,\rho=1$.

The 12 nondiagonal elements which are left should be transformed to the diagonal positions of new density matrix $\rho'=\hat{W}\rho\hat{W}^{\dagger}$, by performing a proper quantum operation $\hat{W}$ on the original density matrix ρ. For example, after a quantum manipulation $\hat{U}_J^{(1)}$, see Eq. (11), evolving the system to $\bar{\rho}=\hat{U}_J^{(1)}\rho\hat{U}_J^{(1)\dagger}$, we can perform the P_{12} measurement to obtain

$$\bar{I}_c^{(12)}\propto\mathrm{tr}[\bar{\rho}\hat{P}_1\otimes\hat{P}_2]=\tfrac{1}{2}[\rho_{01,01}+\rho_{11,11}-2\,\mathrm{Re}(\rho_{01,11})], \tag{18}$$

for determining $\mathrm{Re}(\rho_{01,11})$; and perform the P_1 measurement to obtain

$$\bar{I}_c^{(2)}\propto\mathrm{tr}[\bar{\rho}\hat{P}_1]=\tfrac{1}{2}[1+2\,\mathrm{Re}(\rho_{00,10}-\rho_{01,11})], \tag{19}$$

for determining $\mathrm{Re}(\rho_{00,10})$. All the remaining 10 off-diagonal elements of ρ can be similarly determined.

Table I summarizes such a procedure for tomographic characterization of an unknown two-qubit state in this fixed-coupling two-qubit system. We need to first apply to ρ the quantum operations listed in the first column of Table I. Afterwards, the projective measurements listed in the second column of Table I must be made. In this way, all the matrix

TABLE I. Tomographic characterization of an unknown two-qubit state $\rho=(\rho_{ij,kl})$ with $i,j,k,l=0,1$ in capacitively-coupled Josephson circuits. Each row of this table requires operating on an identically prepared initial state ρ.

Operations	Measurement	Determining
No	P_{12}	$\rho_{11,11}$
No	P_1	$\rho_{10,10}$
No	P_2	$\rho_{01,01}$
$\hat{U}_J^{(1)}$	P_{12}	$\mathrm{Re}(\rho_{01,11})$
$\hat{U}_J^{(1)}$	P_1	$\mathrm{Re}(\rho_{00,10})$
$\hat{U}_J^{(2)}$	P_{12}	$\mathrm{Re}(\rho_{10,11})$
$\hat{U}_J^{(2)}$	P_2	$\mathrm{Re}(\rho_{00,01})$
$\hat{U}_-^{(1)}(\frac{\pi}{4})\hat{U}_+^{(2)}(\frac{\pi}{2})$	P_1	$\mathrm{Re}(\rho_{00,11})$
$\hat{U}_+^{(1)}(\frac{\pi}{4})\hat{U}_+^{(2)}(\frac{\pi}{2})$	P_{12}	$\mathrm{Re}(\rho_{01,10})$
$\hat{U}_-^{(1)}(\frac{\pi}{4})$	P_2	$\mathrm{Im}(\rho_{00,10})$
$\hat{U}_+^{(1)}(\frac{\pi}{4})$	P_2	$\mathrm{Im}(\rho_{01,11})$
$\hat{U}_-^{(2)}(\frac{\pi}{4})$	P_2	$\mathrm{Im}(\rho_{00,01})$
$\hat{U}_+^{(2)}(\frac{\pi}{4})$	P_2	$\mathrm{Im}(\rho_{10,11})$
$\hat{U}_{\mathrm{co}}$	P_{12}	$\mathrm{Im}(\rho_{00,11})$
$\hat{U}_{\mathrm{co}}$	P_2	$\mathrm{Im}(\rho_{01,10})$

elements of ρ can be determined. Of course, this is not a unique approach for determining all fifteen independent elements of the density matrix. In fact, the expected tomographic reconstruction could also be achieved by only using the P_1 and P_2 measurements, and making the P_{12} measurement unnecessary.

With the density matrix ρ obtained by the above tomographic measurements and comparing to the density matrix of ideal Bell states, i.e.

$$\rho_{|\psi_\pm\rangle}=\begin{pmatrix}1&0&0&\pm1\\0&0&0&0\\0&0&0&0\\\pm1&0&0&1\end{pmatrix},\quad \rho_{|\phi_\pm\rangle}=\begin{pmatrix}0&0&0&0\\0&1&\pm1&0\\0&\pm1&1&0\\0&0&0&0\end{pmatrix},$$

the fidelity of the EPR pairs generated above can be defined as $F_{|\psi_\pm\rangle}=\mathrm{tr}(\rho\rho_{|\psi_\pm\rangle})$ and $F_{|\phi_\pm\rangle}=\mathrm{tr}(\rho\rho_{|\phi_\pm\rangle})$, respectively.

So far, we have shown that EPR correlations could be produced between two capacitively coupled Cooper-pair boxes. Further, these entangled states can be characterized by using tomographic techniques via a series of projective measurements. Below, we will numerically estimate the lifetimes of these states and discuss their possible application to test Bell's inequality.

IV. DECAY OF EPR-BELL STATES DUE TO GATE-VOLTAGE NOISE

The EPR pairs generated above are the eigenstates of the Hamiltonian $\hat{H}_{\mathrm{int}}=E_{12}\sigma_z^{(1)}\sigma_z^{(2)}$, and thus are long lived, at least theoretically, in the idle circuit with $E_C^{(j)}=E_J^{(j)}=0$. Under the influence of various disturbing perturbations, these pure quantum states will finally decay to the corresponding mixed states. In fact, experimental solid-state circuits are very sensitive to decoherence because of the coupling to the many degrees of freedom of the solid-state environment. However, coherent quantum manipulations on the generated EPR pairs are still possible if their decay times are sufficiently long.

A. Model

The typical dominating noise in Josephson circuits is caused either by linear fluctuations of the electromagnetic environment (e.g., circuitry and radiation noises) or by low-frequency noise due to fluctuations in various charge or current channels (e.g., the background charge and critical current fluctuations). Usually, the former one behaves as Ohmic dissipation [30] and the latter one produces a $1/f$ spectrum [31], which is still not fully understood in solid-state circuits (see, e.g., [32]). Here, we assume that the decay of the EPR pairs arises from linear environmental noises, i.e., we investigate the fluctuations of the gate voltages applied to the qubits. Moreover, the effect of background charges that cause dephasing are modeled by setting the zero frequency part of the bath spectral function to a value given by the experimentally obtained [33] dephasing rates for the charge qubit system. This approach is valid for noise that can be approximated as leading to an exponential decay. The effect of gate-voltage noise on a single charge qubit has been discussed in [30]. We now study two such noises in a capacitively-coupled circuit. Each electromagnetic environment is treated as a quantum system with many degrees of freedom and modeled by a bath of harmonic oscillators. Furthermore, each of these oscillators is assumed to be weakly coupled to the Cooper-pair boxes.

The Hamiltonian containing the fluctuations of the applied gate voltages can be generally written as

$$\tilde{H}=\hat{H}+\hat{H}_B+\hat{V},$$

with

$$\hat{H}_B=\sum_{j=1,2}\sum_{\omega_j}\left(\hat{a}_{\omega_j}^\dagger\hat{a}_{\omega_j}+\frac{1}{2}\right)\hbar\,\omega_j, \tag{20}$$

and

$$\hat{V}=\sigma_z^{(1)}(X_1+\beta X_2)+\sigma_z^{(2)}(X_2+\gamma X_1), \tag{21}$$

being the Hamiltonians of the two baths and their interactions with the two boxes. Here,

$$X_j=\frac{E_{C_j}C_{g_j}}{4e}\sum_{\omega_j}(g_{\omega_j}^*\hat{a}_{\omega_j}^\dagger+g_{\omega_j}\hat{a}_{\omega_j}), \tag{22}$$

with $\hat{a}_{\omega_j},\hat{a}_{\omega_j}^\dagger$ being the Boson operators of the jth bath, and g_{ω_j} the coupling strength between the oscillator of frequency ω_j and the nondissipative system. Due to the mutual coupling of the two Cooper pair boxes, there will be cross talk of the noise affecting each qubit. This is modeled in the spin-boson model with two bosonic baths represented above by the terms with the additional factors β and γ. The amount of

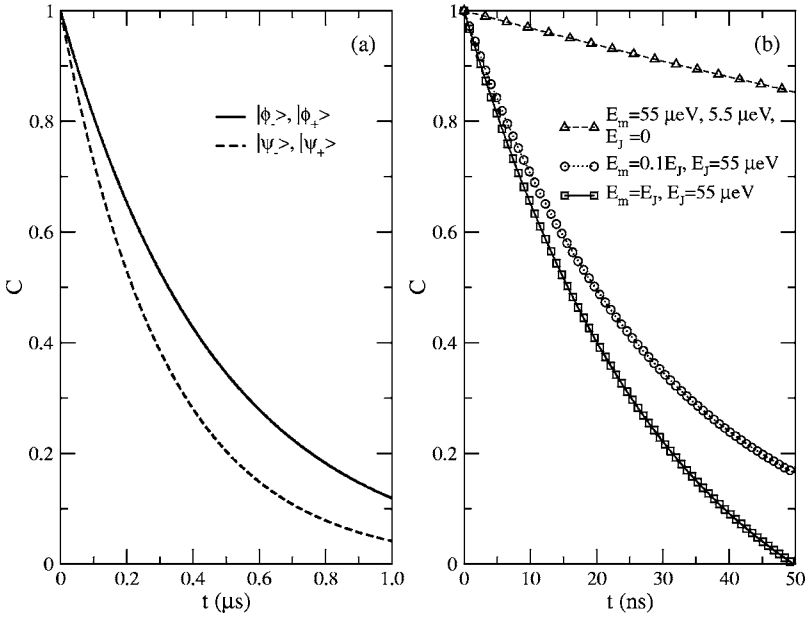

FIG. 2. Simulated time evolution of the concurrence $\mathcal{C}$ for a two-qubit system coupled to a noisy environment and initially prepared in the Bell states. Here, the temperature and the strength of noise are set to $T=10$ mK and $\eta=10^{-3}$, respectively. (a) Captures the long-time decay of the concurrence for different entangled input states in the case of vanishing single-qubit terms, i.e., when only the inter-qubit coupling terms are present. (b) Compares the decays of $|\psi_-\rangle$ for different interbit-couplings ($E_m=E_J$, and $0.1E_J$) without ($E_J^{(1)}=E_J^{(2)}=0$), and with Josephson tunneling ($E_J^{(1)}=E_J^{(2)}=E_J=55$ μeV).

this cross talk is given by the network of capacitances or the corresponding energies only; namely, $\beta=E_m/2E_{C_2}$ and $\gamma=E_m/2E_{C_1}$, and by inserting experimental values one finds that $\beta\approx\gamma\approx 1/10$.

The effects of these noises can be characterized by their power spectra. The spectral density of the voltage noise for Ohmic dissipation can be expressed as

$$J_f(\omega)=\pi\sum_{\omega_j}|g_{\omega_j}|^2\delta(\omega-\omega_j)\sim\eta\hbar\,\omega\omega_c^2/(\omega_c^2+\omega^2). \quad (23)$$

Here, a Drude cutoff with cutoff frequency $\omega_c=10^4$ GHz has been introduced, which is well above all relevant frequency scales of the system and given by the circuit properties [38]. The dimensionless constant η characterizes the strength of the environmental effects. Introducing the impedance, $Z_t(\omega)=1/[i\omega C_t+Z^{-1}(\omega)]$, the spectral function for the fluctuations can be expressed via the environmental impedance $J_f(\omega)=\omega\,\mathrm{Re}[Z_t(\omega)]$. Here, $Z(\omega)\sim R_V$ is the Ohmic resistor and C_t is the total capacitance connected to the Cooper-pair box.

The well-established Bloch-Redfield formalism [22,34] provides a systematic way to obtain a generalized master equation for the reduced density matrix of the system, weakly influenced by dissipative environments. A subtle Markov approximation is also made in this theory such that the resulting master equation is local in time. In the regime of weak coupling to the bath and low temperatures, this theory is numerically equivalent to a full non-Markovian path integral approach [35]. For the present case, a set of master equations are obtained in the eigenbasis of the unperturbed Hamiltonian [30]

$$\dot{\rho}_{nm}=-i\omega_{nm}\rho_{nm}-\sum_{kl}R_{nmk\ell}\rho_{k\ell}, \quad (24)$$

with the Redfield tensor elements $R_{nmk\ell}$ given by

$$R_{nmk\ell}=\delta_{\ell m}\sum_r\Gamma^{(+)}_{nrrk}+\delta_{nk}\sum_r\Gamma^{(-)}_{\ell rrm}-\Gamma^{(-)}_{\ell mnk}-\Gamma^{(+)}_{\ell mnk}, \quad (25)$$

and the rates $\Gamma^{(\pm)}$ given by the Golden Rule expressions

$$\Gamma^{(+)}_{\ell mnk}=\hbar^{-2}\int_0^\infty dt e^{-i\omega_{nk}t}\langle V_{I,\ell m}(t)V_{I,nk}(0)\rangle,$$

$$\Gamma^{(-)}_{\ell mnk}=\hbar^{-2}\int_0^\infty dt e^{-i\omega_{\ell m}t}\langle V_{I,\ell m}(0)V_{I,nk}(t)\rangle.$$

Here, $V_{I,\ell m}(t)$ is the matrix element of the system-bath coupling term of the Hamiltonian in the interaction picture with respect to the bath, and the brackets denote thermal average.

Note again that the strength of the dissipative effects is characterized by the dimensionless parameter η. From experimental measurements of the noise properties of the charge qubit system [36], it is found that the strength of the Ohmic noise is given by

$$\eta=\frac{4e^2R}{\hbar\pi}\approx 1.8\times 10^{-3}, \quad (26)$$

where $R\approx 6\Omega$. Thus, current technology gives a noise floor of approximately $\eta\sim 10^{-3}$, which will be used for the numerical simulations. For visualization of the decay of the Bell states, we compute the concurrence [37], given by

$$\mathcal{C}=\max\{0,\sqrt{\varrho_1}-\sqrt{\varrho_2}-\sqrt{\varrho_3}-\sqrt{\varrho_4}\}. \quad (27)$$

Here, the ϱ_i, $i=1,2,3,4$, are the eigenvalues of $\rho\tilde{\rho}$ with $\tilde{\rho}=(\sigma_y^1\otimes\sigma_y^2)\rho^*(\sigma_y^1\otimes\sigma_y^2)$. The concurrence is a measure for entanglement and indicates non-locality. The maximally entangled Bell states (i.e., the ideal EPR correlations) yield a value of 1, whereas a fully separable state gives 0.

B. Numerical results

The results of the simulations are shown in Fig. 2, where

the time evolution of the concurrence $\mathcal{C}$ shows the decays of all Bell states, for temperature set to an experimentally feasible value of 10 mK. The lifetimes of the operationally idle EPR pairs are of the order of several μs and thus sufficiently long (compared to the duration $\sim$100 ps of the usual quantum manipulation).

For the case where only the coupling term between the qubits is present and all single-qubit terms in the Hamiltonian are suppressed, Fig. 2(a) shows that the Bell states decay exponentially fast to zero: $\mathcal{C}(t)\sim\exp(-At)$, with $A\simeq 2.13\times 10^6$ Hz for $|\phi_\pm\rangle$ and $A\simeq 3.18\times 10^6$ Hz for $|\psi_\pm\rangle$. In this case, only pure dephasing contributes to overall decoherence rates, as $\hat{H}=\hat{H}_{\rm int}=E_{12}\sigma_z^{(1)}\sigma_z^{(2)}$ and $[\hat{H},\hat{V}]=0$, see Ref. [38]. The magnitude of the dephasing part of decoherence is essentially determined by the $1/f$-noise. To model this, a peak in the spectral function at zero frequency can be introduced with a magnitude given by microscopic calculations or experimental measurements of the magnitude of $1/f$ noise in these qubit structures. However, note that often the noise leads to nonexponential decay, which can neither be modeled by Bloch-Redfield theory nor be parametrized by a single rate. Here, we assume Markovian and Gaussian noise and set the zero frequency contribution, i.e., the dephasing due to the $1/f$ noise to an experimentally reported value of $\Gamma_\varphi\approx 10^7$ Hz [33]. Note that the individual contributions from different noise sources sum up in the spectral function $J_\Sigma(\omega)=J_f(\omega)+J_{1/f}(\omega)$, which also holds at $\omega=0$. It is interesting to note that the decay time is independent of the interqubit coupling strength E_{12}. In more detail, when the coupling energy E_{12} in the Hamiltonian is increased the decay does not change. The reason for this behavior is that the pure dephasing is only affected by the zero frequency part of the spectrum, which is obviously independent of the individual frequency splittings, i.e., the characteristic energy scale of the Hamiltonian. Also, one of the most important results, namely that the decay time of $|\phi_\pm\rangle$ is longer than that of $|\psi_\pm\rangle$, is consistent with the analog experimental one in ion traps [9]. This is because $|\phi_\pm\rangle$ is the superposition of the two states with the same energy, while $|\psi_\pm\rangle$ corresponds to higher energy and is more sensitive to such perturbations.

When the Josephson-tunneling terms exist, e.g., $E_J^{(1)}=E_J^{(2)}=E_J$, we see from Fig. 2(b) that the decays of the generated EPR pairs are significantly faster than in the former case without any tunneling. This is because the additional Josephson tunneling provides additional decoherence channels since the Hamiltonian of the circuit now does not commute with the couplings to the baths. Moreover, also the overall energy scale in the Hamiltonian increases. In this case, the weaker interbit-coupling corresponds to the slower decay of the EPR pairs.

V. TESTING BELL'S INEQUALITY

A possible application of the deterministically generated EPR pairs is to test BI at the macroscopic level. Due to the existence of interbit constant coupling, the required local operations of encoding classical information $\{\theta_j\}$ into the EPR pairs cannot be strictly implemented. In Ref. [21] we proposed an approach to overcome this difficulty by introducing the effective single-qubit operations including corrections due to the constant coupling. Instead, here we approximately perform the encoding procedure by sequentially applying the conditional single-qubit operations $\bar{U}_J^{(j)}$, $(j=1,2)$ in Eq. (10). For the case of $\alpha_1=\alpha_2=\alpha$, the validity of the above quasilocal encodings could be described by the variation of the degree of entanglement (i.e., concurrence) of the EPR pairs, e.g., $|\psi_\pm\rangle$

$$\Delta\mathcal{C}=1-\sqrt{1-[\sin(2\alpha)(1-\cos(2\varphi_1+2\varphi_2))/2]^2}, \quad (28)$$

with $\varphi_j=2\gamma_j t/\hbar$. Obviously, $\Delta\mathcal{C}=0$ corresponds to the ideal locality or maximal locality. After the above encoding, we simultaneously detect [13] the populations of qubits and check if they are in the same logic states: the excited one $|1\rangle$ or the ground state $|0\rangle$.

Theoretically, the correlation of two local variables, φ_1 and φ_2, can be defined as the expectation value of the operator $\hat{P}_T=|11\rangle\langle 11|+|00\rangle\langle 00|-|10\rangle\langle 10|-|01\rangle\langle 01|=\hat{\sigma}_z^{(1)}\otimes\hat{\sigma}_z^{(2)}$ and reads

$$E(\varphi_1,\varphi_2)=\cos^2\alpha+\sin^2\alpha\cos(\varphi_1+\varphi_2). \quad (29)$$

Experimentally, all the above operational steps can be repeated many times in a controllable way for various parameter sets. As a consequence, the correlation function E can be measured by

$$E(\varphi_1,\varphi_2)=\frac{N_{\rm same}(\varphi_1,\varphi_2)-N_{\rm diff}(\varphi_1,\varphi_2)}{N_{\rm same}(\varphi_1,\varphi_2)+N_{\rm diff}(\varphi_1,\varphi_2)}, \quad (30)$$

for any pair of chosen classical variables φ_1 and φ_2. Here, $N_{\rm same}(\varphi_1,\varphi_2)$ ($N_{\rm diff}(\varphi_1,\varphi_2)$) are the number of events with two qubits found in the same (different) logic states. With these measured correlation functions, one can experimentally test the BI in the present superconducting systems.

We consider the following typical set of angles: $\{\varphi_j,\varphi_j'\}=\{-\pi/8,3\pi/8\}$ and the interbit couplings $E_m=4E_{12}=E_J$, $E_J/10$, and $E_J/100$, respectively. The corresponding variations $\Delta\mathcal{C}$ of the concurrence and the correlation $E(\varphi_1,\varphi_2)$, which yields the Clauser, Horne, Shimony, and Holt (CHSH) [3] function $f=|E(\varphi_1,\varphi_2)+E(\varphi_1',\varphi_2)+E(\varphi_1,\varphi_2')-E(\varphi_1',\varphi_2')|$, are given in Table II. It is seen that the variations $\Delta\mathcal{C}$ of the concurrence, after the above quasilocal operations $\bar{U}_J^{(j)}$, decrease with decreasing interbit coupling. For very weak coupling, e.g., $E_m/E_J=0.1$ (or 0.01), the applied conditional single-qubit operations can be regarded as local, away from 0.4%, (or 0.004%). Besides these tiny loopholes of locality, Table II shows that the CHSH-type Bell's inequality [3]

$$f<2 \quad (31)$$

is obviously violated.

VI. DISCUSSION AND CONCLUSION

Similar to other theoretical schemes (see, e.g., Ref. [18]) the realizability of the present proposal also faces certain technological challenges, such as the rapid switching of the

TABLE II. Variations of the concurrence, $\Delta\mathcal{C}$, correlations E, and CHSH-functions f, for certain typical parameters of the interbit coupling E_m and the controllable classical variables φ_1 and φ_2.

E_m	(φ_1,φ_2)	$\Delta\mathcal{C}$	$E(\varphi_1,\varphi_2)$	f
E_J	$(-\pi/8,-\pi/8)$	0.006 99	0.765 69	
	$(-\pi/8,3\pi/8)$	0.006 99	0.765 69	2.6627
	$(3\pi/8,-\pi/8)$	0.006 99	0.765 69	
	$(3\pi/8,3\pi/8)$	0.269 43	−0.365 69	
$E_J/10$	$(-\pi/8,-\pi/8)$	0.002 38	0.724 34	
	$(-\pi/8,3\pi/8)$	0.000 11	0.707 84	2.8264
	$(3\pi/8,-\pi/8)$	0.000 11	0.707 84	
	$(3\pi/8,3\pi/8)$	0.003 63	−0.702 85	
$E_J/100$	$(-\pi/8,-\pi/8)$	0.000 01	0.707 11	
	$(-\pi/8,3\pi/8)$	0.000 01	0.707 11	2.8284
	$(3\pi/8,-\pi/8)$	0.000 01	0.707 11	
	$(3\pi/8,3\pi/8)$	0.000 04	−0.707 06	

charge and Josephson energies of the SQUID-based qubits and decoherence due to the various environmental noises. Our numerical results, considering various typical fluctuations, showed that the lifetime of the generated EPR pairs adequately allows to perform the required operations for experimentally testing Bell's inequality. Indeed, for current experiments [12], the decay time of a *two*-qubit excited state is as long as $\sim$0.6 ns, even for the very strong interbit coupling, e.g., $E_m \simeq E_J$. Longer decoherence times are possible for weaker interbit couplings. In addition, for testing this, the influence of the environmental noises and operational imperfections is not fatal, as the nonlocal correlation $E(\varphi_i,\varphi_j)$ in Bell's inequality is statistical—its fluctuation could be effectively suppressed by the averages of many repeatable experiments.

In summary, for the experimentally realized capacitively coupled Josephson nanocircuits, we found that several typical two-qubit quantum operations (including simultaneously flipping the two qubits and only evolving a selected qubit in the case of leaving the other one unchanged) could be easily implemented by properly setting the controllable parameters of circuits, e.g., the applied gate voltages and external fluxes. As a consequence of this, macroscopic EPR correlated pairs could be deterministically generated from the ground state $|00\rangle$ by two conditional single-qubit operations: prepare the superposition of the two logic states of a selected qubit, and then only flip one of the two qubits. To experimentally confirm the proposed generation schemes, we also propose an effective tomographic technique for determining all density matrix elements of the prepared states by a series of quantum projective measurements. The deterministically generated EPR pairs provide an effective platform to test, at the macroscopic level, certain fundamental principles, e.g., the nonlocality of quantum entanglement via violating the Bell's inequality.

The approach proposed here can be easily modified to engineer quantum entanglement in other "fixed-interaction" solid-state systems, e.g., capacitively (inductively) coupled Josephson phase (flux) system and Ising (Heisenberg)-spin chains.

ACKNOWLEDGMENTS

We acknowledge useful discussions with J. Q. You, J. S. Tsai, O. Astafiev, S. Ashhab, and F. K. Wilhelm. M.J.S gratefully acknowledges financial support of RIKEN and the DFG through SFB 631. This work was supported in part by the National Security Agency (NSA) and Advanced Research and Development Activity (ARDA) under Air Force Office of Research (AFOSR) Contract No. F49620-02-1-0334; and also supported by the National Science Foundation Grant No. EIA-0130383.

[1] A. Einstein, B. Podolsky, and N. Rosen, Phys. Rev. **47**, 777 (1935).
[2] J. Bell, Physics (Long Island City, N.Y.) **1**, 195 (1964).
[3] See, e. g., G. Weihs, T. Jennewein, C. Simon, H. Weinfurter, and A. Zeilinger, Phys. Rev. Lett. **81**, 5039 (1998); A. Aspect, J. Dalibard, and G. Roger, *ibid.* **49**, 1804 (1982); W. Tittel, J. Brendel, H. Zbinden, and N. Gisin, *ibid.* **81**, 3563 (1998).
[4] A. Bramon and M. Nowakowski, Phys. Rev. Lett. **83**, 1 (1999).
[5] B. J. Oliver and C. R. Stroud, Jr., J. Opt. Soc. Am. B **4**, 1426 (1987); J. I. Cirac and P. Zoller, Phys. Rev. A **50**, R2799 (1994).
[6] R. Ionicioiu, P. Zanardi, and F. Rossi, Phys. Rev. A **63**, 050101(R) (2001).
[7] L. F. Wei and F. Nori, Europhys. Lett. **65**, 1 (2004); L. F. Wei, Yu-xi Liu, and F. Nori, Phys. Rev. A **70**, 063801 (2004); E. Solano, R. L. de Matos Filho, and N. Zagury, Phys. Rev. A **59**, R2539 (1999).
[8] E. Hagley, X. Maitre, G. Nogues, C. Wunderlich, M. Brune, J. M. Raimond, and S. Haroche, Phys. Rev. Lett. **79**, 1 (1997).
[9] C. F. Roos, G. P. T. Lancaster, M. Riebe, H. Häffner, W. Hänsel, S. Gulde, C. Becher, J. Eschner, F. Schmidt-Kaler, and R. Blatt, Phys. Rev. Lett. **92**, 220402 (2004).
[10] M. A. Rowe, D. Kiepinski, V. Meyer, C. A. Sackett, W. M. Itano, C. Monroe, and D. J. Wineland, Nature (London) **409**, 791 (2001).
[11] D. L. Moehring, M. J. Madsen, B. B. Blinov, and C. Monroe, Phys. Rev. Lett. **93**, 090410 (2004).
[12] Yu. P. Pashkin, T. Yamamoto, O. Astafiev, Y. Nakamura, D. V. Averin, and J. S. Tsai, Nature (London) **421**, 823 (2003).
[13] R. McDermott, R. W. Simmonds, M. Steffen, K. B. Cooper, K. Cicak, K. D. Osborn, S. Oh, D. P. Pappas, and J. M. Martinis, Science **307**, 1299 (2005).
[14] A. J. Berkley, H. Z. Xu, R. C. Ramos, M. A. Gubrud, F. W. Strauch, P. R. Johnson, J. R. Anderson, A. J. Dragt, and C. J. Lobb, F. C. Wellstood, Science **300**, 1548 (2003); H. Xu, F. W.

Strauch, S. K. Dutta, P. R. Johnson, R. C. Ramos, A. J. Berkley, H. Paik, J. R. Anderson, A. J. Dragt, C. J. Lobb, and F. C. Wellstood, Phys. Rev. Lett. **94**, 027003 (2005); G. P. Berman, A. R. Bishop, D. I. Kamenev, and A. Trombettoni, Phys. Rev. B **71**, 014523 (2005).

[15] A. Blais, A. Maassen van den Brink, and A. M. Zagoskin, Phys. Rev. Lett. **90**, 127901 (2003).

[16] L. F. Wei, Yu-xi Liu, and F. Nori, Europhys. Lett. **67**, 1004 (2004); Phys. Rev. B **71**, 134506 (2005).

[17] H. Tanaka, Y. Sekine, S. Saito, and H. Takayanagi, Supercond. Sci. Technol. **14**, 1161 (2001).

[18] Y. Makhlin, G. Schön, and A. Shnirman, Nature (London) **398**, 305 (1999); J. Q. You, J. S. Tsai, and F. Nori, Phys. Rev. Lett. **89**, 197902 (2002).

[19] J. Q. You and F. Nori, Phys. Rev. B **68**, 064509 (2003); G. P. He, S. L. Zhu, Z. D. Wang, and H. Z. Li, Phys. Rev. A **68**, 012315 (2003).

[20] J. Q. You, J. S. Tsai, and F. Nori, Phys. Rev. B **68**, 024510 (2003).

[21] L. F. Wei, Yu-xi Liu, and F. Nori, Phys. Rev. B **72**, 104516 (2005).

[22] P. N. Argyres and P. L. Kelley, Phys. Rev. **134**, A98 (1964).

[23] T. Yamamoto, Yu. P. Pashkin, O. Astafiev, Y. Nakamura, and J. S. Tsai, Nature (London) **425**, 941 (2003).

[24] X. X. Zhou, Z. W. Zhou, G. C. Guo, and M. J. Feldman, Phys. Rev. Lett. **89**, 197903 (2002); Z. W. Zhou, B. Yu, X. X. Zhou, M. J. Feldman, and G. C. Guo, *ibid.* **93**, 010501 (2004).

[25] A. Barenco, C. H. Bennett, R. Cleve, D. P. DiVincenzo, N. Margolus, P. Shor, T. Sleator, J. A. Smolin, and H. Weinfurter, Phys. Rev. A **52**, 3457 (1995).

[26] I. L. Chuang, N. Gershenfeld, M. G. Kubinec, and D. Leung, Proc. R. Soc. London, Ser. A **454**, 447 (1998).

[27] A. G. White, D. F. V. James, W. J. Munro, and P. G. Kwiat, Phys. Rev. A **65**, 012301 (2001); A. G. White, D. F. V. James, P. H. Eberhard, and P. G. Kwiat, Phys. Rev. Lett. **83**, 3103 (1999).

[28] Yu-xi Liu, L. F. Wei, and F. Nori, Europhys. Lett. **67**, 874 (2004); Phys. Rev. B **72**, 014547 (2005).

[29] Y. Nakamura, Yu. A. Pashkin, and J. S. Tsai, Nature (London) **398**, 786 (1999).

[30] U. Weiss, *Quantum Dissipative Systems*, 2nd edition (World Scientific, Singapore, 1999); Y. Makhlin, G. Schön, and A. Shnirman, Rev. Mod. Phys. **73**, 357 (2001).

[31] A. Shnirman, G. Schön, I. Martin, and Y. Makhlin, Phys. Rev. Lett. **94**, 127002 (2005); E. Paladino, L. Faoro, G. Falci, and R. Fazio, *ibid.* **88**, 228304 (2002).

[32] H. Gutmann, F. K. Wilhelm, W. M. Kaminsky, and S. Lloyd, Phys. Rev. A **71**, 020302(R) (2005); G. Falci, A. D'Arrigo, A. Mastellone, and E. Paladino, Phys. Rev. Lett. **94**, 167002 (2005).

[33] O. Astafiev (private communication).

[34] M. C. Goorden and F. K. Wilhelm, Phys. Rev. B **68**, 012508 (2003).

[35] L. Hartmann, I. Goychuk, M. Grifoni, and P. Hänggi, Phys. Rev. E **61**, R4687 (2000).

[36] O. Astafiev, Yu. A. Pashkin, Y. Nakamura, T. Yamamoto, and J. S. Tsai, Phys. Rev. Lett. **93**, 267007 (2004).

[37] W. K. Wootters, Phys. Rev. Lett. **80**, 2245 (1997).

[38] M. J. Storcz and F. K. Wilhelm, Phys. Rev. A **67**, 042319 (2003).